

## Article

# Mechanical Characterization of the Frozen and Thawed States of Coal after the Action of LN<sub>2</sub> at In Situ Formation Pressure

Lei Qin <sup>1,2,\*</sup> , Pengfei Liu <sup>1,2</sup>, Hui Wang <sup>1,2</sup>, Botao Li <sup>1,2</sup>, Ruizhe Wang <sup>1,2</sup>, Jiawei Li <sup>1,2</sup>, Rongwei Luo <sup>1,2</sup> and Shiyin Lv <sup>1,2</sup>

<sup>1</sup> College of Safety Science and Engineering, Xi'an University of Science and Technology, Xi'an 710054, China; 15379115465@163.com (P.L.); wanghui31920@163.com (H.W.); 20120089021@stu.xust.edu.cn (B.L.); wruiizhe@yeah.net (R.W.); lijiawei0118jw@163.com (J.L.); lrongwei0113@163.com (R.L.); lv\_shiyin@163.com (S.L.)

<sup>2</sup> Key Laboratory of Ministry of Education for Western Mine Exploitation and Hazard Prevention, Xi'an University of Science and Technology, Xi'an 710054, China

\* Correspondence: qinlei@xust.edu.cn

**Abstract:** Coal penetration enhancement technology is the key to increase the production of coalbed methane. Coal bodies are subjected to different peripheral pressures in the in situ strata, and the study of the changes in the mechanical strength of coal bodies under different peripheral pressures after the action of liquid nitrogen is crucial for the penetration enhancement of liquid nitrogen (LN<sub>2</sub>)-fractured coal. In this paper, an MTS universal testing machine was utilized to carry out experiments to obtain the stress–strain curves of the coal under different freezing times under 1 MPa surrounding pressure and different surrounding pressures after 50 min of LN<sub>2</sub> action. The experimental results showed the following: (1) the uniaxial compressive strength and peak strain of coal samples in a frozen state are positively correlated under two conditions. The modulus of elasticity decreased before 100 min at different times of LN<sub>2</sub> action, and the modulus of elasticity was maximum at 5 MPa at different peripheral pressure actions; (2) the uniaxial compressive strength and peak strain of the frozen-thawed coal samples decreased before 100 min of LN<sub>2</sub> action at different times, and the modulus of elasticity continued to decrease. The uniaxial compressive strength and modulus of elasticity of coal samples in freeze–thaw state under different peripheral pressures were the largest at 5 MPa, and the peak strain was negatively correlated. (3) The elastic strain energy of the frozen coal samples under the action of LN<sub>2</sub> at different times was positively correlated with the freezing time before 80 min, and negatively correlated after 80 min. The elastic strain energy of the frozen coal samples was positively correlated with the freezing time. The elastic strain energy and freezing time of the two coal samples under different circumferential pressures were positively correlated before 5 MPa and negatively correlated after 5 MPa, with opposite dissipation energies. (4) The water–ice phase transition and temperature–thermal stresses on the internal structure of the coal in the presence of LN<sub>2</sub> cause significant damage. The degradation of coal samples in the freeze–thaw state is even higher under in situ ground pressure.

**Keywords:** LN<sub>2</sub> fracturing; different siege pressures; different freezing states; mechanical properties; energy evolution



**Citation:** Qin, L.; Liu, P.; Wang, H.; Li, B.; Wang, R.; Li, J.; Luo, R.; Lv, S. Mechanical Characterization of the Frozen and Thawed States of Coal after the Action of LN<sub>2</sub> at In Situ Formation Pressure. *Processes* **2024**, *12*, 299. <https://doi.org/10.3390/pr12020299>

Academic Editor: Raymond Cecil Everson

Received: 29 December 2023

Revised: 28 January 2024

Accepted: 28 January 2024

Published: 30 January 2024



**Copyright:** © 2024 by the authors. Licensee MDPI, Basel, Switzerland. This article is an open access article distributed under the terms and conditions of the Creative Commons Attribution (CC BY) license (<https://creativecommons.org/licenses/by/4.0/>).

## 1. Introduction

As an important support for China's economic development, coal has always occupied a dominant position in the energy structure [1,2]. Coalbed methane (CBM) is often generated along with the coal mining process [3–5]. The geological characteristics of coal seams in China are complex, and most of the coal seams are characterized by “low permeability, high adsorption and high stress” [6–8]. Coal bed methane (CBM) extraction is difficult, and coal bed penetration enhancement technology has become the key to improving the efficiency of CBM extraction [9,10]. Coal bodies are mostly in a three-way stress state under

in situ formation pressure, and it is difficult to characterize the real stress state of coal bodies in conventional uniaxial compression experiments, so the technology of simulating the fracturing and penetration of coal seams under in situ formation pressure is crucial for improving the efficiency of coalbed methane extraction.

With the continuous development of unconventional natural gas development technology, the limitations of traditional hydraulic fracturing, such as high pollution and high water demand, are becoming more and more prominent. In recent years, anhydrous cryogenic fracturing technology represented by LN<sub>2</sub> fracturing [11,12] and supercritical CO<sub>2</sub> fracturing [13] has developed rapidly. Among them, LN<sub>2</sub> fracturing technology has been given attention by a large number of scholars because of the low temperature of LN<sub>2</sub>, and the water–ice phase transition and liquid–gas phase transition expansion characteristics [14]. At atmospheric pressure, LN<sub>2</sub> can reach a temperature of  $-196\text{ }^{\circ}\text{C}$ , with a latent heat of vaporization of 5.56 kJ/mol. One cubic meter of LN<sub>2</sub> expands to 696 cubic meters of gaseous nitrogen at an atmospheric pressure of 21 °C, generating an enormous expansion force. At the same time, the existing pore water in the coal will freeze rapidly, which will produce a volume expansion of about 9% during the LN<sub>2</sub> vaporization process and generate a freezing expansion force of up to 207 MP. After exposure to LN<sub>2</sub>, the coal samples will be damaged by the effects of cryogenic damage, vaporization expansion of LN<sub>2</sub>, and phase change expansion of water–ice [15,16]. Memon et al. [17] explored the physical and mechanical properties of shale by LN<sub>2</sub> and by heat shocking the shale, using tests such as core expulsion and nanoindentation techniques. In the study of Hou P. et al. [18], who used three states of coal samples for a comparative study of uniaxial compression, Brazilian cleavage after the characteristics of the results showed that the effect of LN<sub>2</sub> treatment on the coal destruction is more obvious, showing the mechanical properties of further deterioration. Du M.L. et al. [19] used a combination of experimental study techniques such as scanning electron microscopy and numerical simulations to analyze the change characteristics of sandstone and coal after LN<sub>2</sub> treatment from the perspective of thermal stress transfer. Cai C.Z. et al. [20] found that LN<sub>2</sub>-contacting coal continuously produces fracturing and internal damage, by studying the AE parameter characteristics, p-wave wave speed change and mechanical characteristics after uniaxial compression after the thermal impact of LN<sub>2</sub> on coal, which has a very important effect on the increase in the permeability of coal. Wang X.Q. et al. [21] carried out experiments based on a triaxial compression system to study the change rule of fractures in coal with different water contents, and the results showed that the original fractures of coal were developed after LN<sub>2</sub> cold dipping, and the expansion of surface fractures was positively correlated with the internal damage. Su S.J. et al. [22] studied the pore distribution, connectivity, and pore evolution characteristics of coal bodies before and after uniaxial compression from the point of view of fractal dimension, and the results showed that the porosity of the coal increased after LN<sub>2</sub> treatment, connectivity increased, and the fissure network was expanded and became more complex. Coal has non-homogeneous pore structures that exhibit anisotropy in their strength and properties [23,24], and internal temperature stresses are altered when the interior is subjected to LN<sub>2</sub> freezing or freeze–thaw treatment. After entering the interior of the coal, LN<sub>2</sub> is converted from liquid to gas, and the gas expands in the pore fractures at different scales. Moisture inside the coal mass comes in contact with LN<sub>2</sub> and undergoes expansion in volume as it transforms from water to ice [25–27]. Based on this, the coal produces different degrees of deformation, the internal pores are developed, a more complex pore fracture network is formed, its internal gas mobility is increased, and the coalbed methane transport is enhanced; through this, the mechanism of LN<sub>2</sub> action can be explored [28].

At present, the research on the mechanical deterioration of LN<sub>2</sub>-fractured coal mainly focuses on the evolution of the mechanical properties of the coal after LN<sub>2</sub> freezing and thawing, and there are fewer investigations on the mechanical properties of the coal after the action of LN<sub>2</sub> under different in situ stratigraphic pressures. In this paper, from the simulation of in situ stratum pressure and LN<sub>2</sub> fracturing, uniaxial compression experi-

ments were carried out on two kinds of coal samples in the freezing state and freezing and thawing state, to obtain the rule of the change in the mechanics of the coal samples in different states, and to provide experimental bases for the study of LN<sub>2</sub> fracturing and penetration enhancement.

## 2. Test Samples and Methods

### 2.1. Coal Sample Collection and Preparation

This experiment was conducted on Yuanzhuang bituminite from Huaibei, Anhui Province, China. Firstly, the core sampler was utilized to make the coal samples into a columnar coal with a diameter-to-height ratio of 2:1 and a 50 mm × 100 mm cylinders, which were dried. The number of coal samples made was 13. In order to minimize the variability of the coal samples, all coal samples were taken from the same seam at similar locations, and obvious cuttings and fractures were avoided when making samples. Finally, the basic parameters of the samples were determined according to the “Coal Micro classification and Mineral Determination Methods” and “Industrial Analysis Methods-Instrumental Methods”, and the results are shown in Table 1.

**Table 1.** Maceral analysis and proximate of the coal samples used in this study.

Coal	Proximate (wt %)				R <sub>o,max</sub> (%)	Maceral Composition (vol %)			
	M <sub>ad</sub>	A <sub>ad</sub>	V <sub>ad</sub>	FC <sub>ad</sub>		V	I	E	M
Bituminite	9.42	7.99	39.37	43.22	1.35	73.14	24.85	0.27	1.74

Notes: M<sub>ad</sub>, moisture, air-drying basis; A<sub>ad</sub>, ash yield, air-drying basis; V<sub>ad</sub>, volatile, air-drying basis; FC<sub>ad</sub>, fixed carbon content, air-drying basis; V, vitrinite; I, inertinite; E, exinite; M, minerals; R<sub>o,max</sub>, vitrinite reflectance.

### 2.2. Experimental Procedure

The main factors controlling the action of LN<sub>2</sub> include enclosure pressure and freezing time. Firstly, the made coal samples were grouped and numbered, dried, and vacuum-saturated with water by a water-saturated machine for 48 h. The water-saturated coal samples were subjected to LN<sub>2</sub> freezing and freeze–thawing treatments at different peripheral pressures using the Seepage Creep and Mechanics Experiment System (SCEMES) in a low-temperature environment. The LN<sub>2</sub>-treated portion of the coal samples were thawed at room temperature for 12 h to complete the freeze–thawing of the coal samples. Then, a total of 7 coal sample loading experiments were carried out after different LN<sub>2</sub> action times under 1 MPa peripheral pressure, and a total of 6 coal sample loading experiments under different peripheral pressures after 50 min of LN<sub>2</sub> action. The LN<sub>2</sub> freezing time was 0 min, 50 min, 100 min, and 150 min, in that order. The different enclosure pressures were 1 MPa, 5 MPa, and 10 MPa in order, and the triaxial compressive tests were carried out under different enclosure pressures after the treatment was completed. The experimental flow is shown in Figure 1. The main parts of the experimental equipment are as follows:

- (1) Vacuum saturator: BSJ intelligent vacuum saturator. The precision of vacuum value is ±0.001 MPa, and the power of the whole machine is 300 W.
- (2) Constant temperature drying oven: LS-101 constant temperature drying oven; temperature range +10–+250 °C.
- (3) LN<sub>2</sub> tank: YDZ-50-A self-pressurized LN<sub>2</sub> tank. The volume is 50 L and the standard working pressure is 0.05 MPa.
- (4) Mechanical performance test equipment: MTS electro-hydraulic servo universal testing machine, model C64.605. The test was performed using axial displacement control with a displacement rate of 0.005 mm/s. Data were collected using MTS PowerTest V5.0 Test Software.

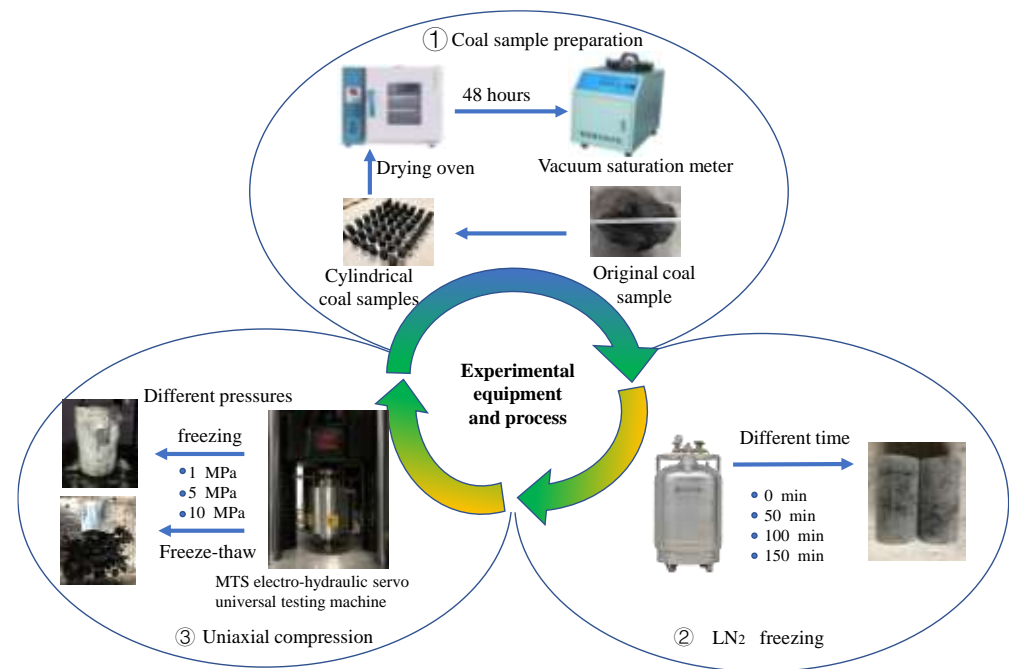


**Figure 1.** Coal sample selection and pretreatment.

### 3. Results

#### 3.1. Changes in Uniaxial Compressive Strength of Coal after LN<sub>2</sub> Treatment at Different Times with the Same Circumferential Pressure

The uniaxial compressive strength of a coal is the ultimate destructive strength of a coal when compression damage occurs under axial stress [29]. Through the change in the ultimate destructive strength, we can obtain the damage situation of coal after LN<sub>2</sub> treatment, and then analyze the effect of LN<sub>2</sub> on coal. Coal is a natural porous structure, there are many initial microporous fractures inside, and under the joint action of LN<sub>2</sub> low-temperature damage fracturing, freezing expansion fracturing, and expansion deformation fracturing, different degrees of microporous fractures are generated inside the coal. During load compression, the pore fissures are compacted and closed under pressure, and the compression fissures are re-generated in the coal samples under continuous load compression, and finally the internal microscopic pores are connected to each other and penetrated, the strength of the coal decreases, and the fissures on the surface of the specimen are shown at the macroscopic level until the destruction of the specimen. LN<sub>2</sub> fracturing treatment of coal samples was used at different times, at which time the degree of internal damage of coal samples was different. The degree of internal fissure development was also different between the frozen-state (TD) coal samples and the freeze-thawed-state (TR) coal samples, and after uniaxial compression, the uniaxial compressive strengths of the coal samples after the action of different LN<sub>2</sub> can be obtained, as shown in Figure 2.

Figure 2 shows the uniaxial compressive stress–strain curves of the frozen-state (TD) coal samples and frozen-thawed state (TR) coal samples treated with LN<sub>2</sub> for different times under 1 MPa circumferential pressure. From Figure 2a, it can be seen that the uniaxial compressive strength of the original coal sample was 5.074 MPa, and the uniaxial compressive strength of the coal samples after 50 min, 100 min and 150 min of LN<sub>2</sub> freezing were 13.014 MPa, 13.778 MPa and 20.435 MPa, which were increased by 200.6%, 171.5%, and 302.7%, respectively, compared with the original coal samples. From Figure 2b, it can be seen that the uniaxial compressive strengths of the coal samples were 3.863 MPa, 4.937 MPa, and 5.507 MPa after 50 min, 100 min, and 150 min of LN<sub>2</sub> freezing and thawing, respectively, which were changed by 23.9%, 2.7%, and 0.3% compared with that of the original coal samples, respectively.

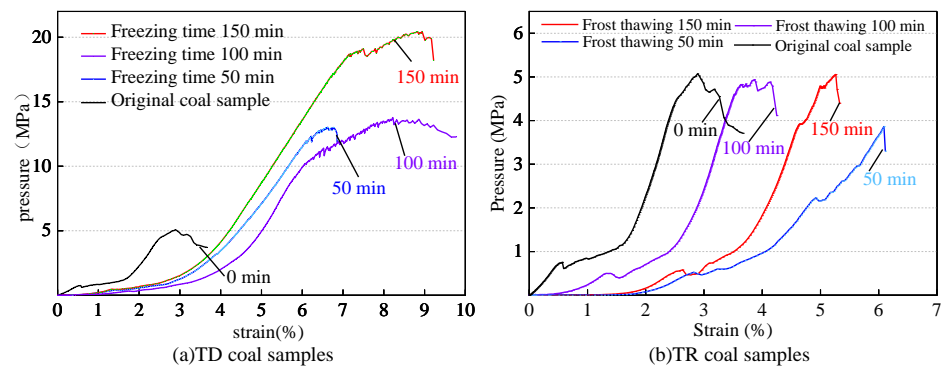


**Figure 2.** Stress–strain curves of TD and TR coal samples after different time treatments with the same enclosure pressure.

### 3.2. Changes in Uniaxial Compressive Strength of Coal after LN<sub>2</sub> Treatment with Different Circumferential Pressure at the Same Time

The coal samples were treated with LN<sub>2</sub> the internal structure was damaged, more fissures were produced, the coal body's ability to resist deformation was reduced, and different mechanical characteristics were shown under different enclosure pressures. In this paper, we mainly carried out the research on the coal samples in the frozen and thawed state, so we did not analyze the stress–strain curves of the raw coal under different enclosing pressures. The test results are shown in Figure 3.

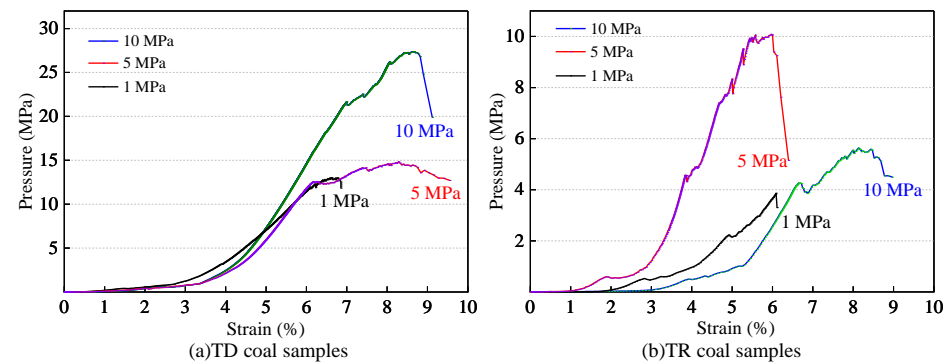


**Figure 3.** Stress–strain curves of coal samples in different states after different circumferential pressure treatments.

Figure 3 shows the uniaxial compressive stress–strain curves of the frozen-state (TD) and frozen–thawed state (TR) coal samples under different peripheral pressures after 50 min of LN<sub>2</sub> treatment. From Figure 3a, it can be seen that the uniaxial compressive strengths of the frozen state coal samples were 13.014 MPa, 14.846 MPa, and 27.380 MPa under the peripheral pressures of 1 MPa, 5 MPa, and 10 MPa. From Figure 3b, the uniaxial compressive strengths of the freeze–thawed coal samples at 1 MPa, 5 MPa, and 10 MPa perimeter pressure were 3.863 MPa, 10.836 MPa, and 5.640 MPa. After the LN<sub>2</sub>-action-saturated water coal samples, with the increase in freezing time, the temperature of the coal samples gradually decreased from the surface to the interior, and the frost structure could be observed on the surface of the coal. The pore water inside the coal was slowly frozen until it was completely frozen, from pore water to pore ice, the pore was filled, and the internal open space was reduced while the pore ice was adhered to the coal. The strength of the coal was “jagged growth” and was strengthened under the continuous action of the ultra-low temperature. The coal matrix was gradually contracted by cold, and when the fissure expansion encountered the coal matrix, the local stress was concentrated and a greater load was required to rupture the coal matrix, which manifested as an increase in the uniaxial compressive strength of the coal. In the process of thawing at room temperature,

the temperature of the coal gradually rose from the outside to the inside, the pore ice in the pores was transformed into pore water, the original fissures were no longer filled, the internal open space was expanded, and the thawed water partly entered the newborn pores and partly flowed out of the coal. Pore expansion due to the temperature stress, water–ice phase change, and LN<sub>2</sub> phase change caused internal stresses to change and the strength of the coal to decrease. The coal matrix was also damaged because of the dual temperature effect of cooling and warming caused by the contraction and expansion of the volume of the coal matrix, resulting in different sizes of shear stress; as a result, the mechanical properties of the coal were affected and reduced.

## 4. Analysis and Discussion

### 4.1. Analysis of Mechanical Properties

#### 4.1.1. Compressive Strength Law Analysis

The excellent fracturing property of LN<sub>2</sub> makes the mechanical parameters, such as the compressive strength of the coal samples, change after the freezing and thawing of LN<sub>2</sub>. The research of related scholars found that LN<sub>2</sub> freezing and freezing and thawing destroyed the pores and fissures of the coal, which led to a decrease in the bearing capacity of the coal and a change in compressive strength [30]. The mechanical strength of the water-saturated coal samples increased in the freezing state, and the mechanical strength of coal decreased in the freeze–thaw-cycle state [31].

The uniaxial compression process of the coal samples under different circumferential pressures all experienced a gradual process of four stages: initial fracture compaction, elastic deformation, plastic deformation, and damage destruction. In the initial fracturing stage, there were fractures inside the coal samples after LN<sub>2</sub> treatment. As the stress increased, the pores gradually decreased until they were compacted and closed, and the stress–strain curve shows a nonlinear slow growth. Entering the elastic deformation stage, the coal sample was further compacted and elastically deformed within the elastic limit as the stress continued to increase; at this time no new fractures were generated and the stress–strain curve grows approximately linearly. As deformation exceeded the elastic limits of the coal sample, new fractures and fissures began to develop internally. As the loading continues, the fractures continued to develop through; the stress–strain curve is no longer linear, showing a “sawtooth” growth characteristic into the yield stage when the coal sample produced plastic deformation until it reaches the peak strength. Finally, the fracture penetration formed a macroscopic representation on the surface of the coal sample, and the coal sample entered the destruction stage.

The change rule of the uniaxial compressive strength of coal samples in the freeze–thaw state and frozen state at different time and under different circumferential pressure can be seen in Figure 4. For the frozen-state (TD) coal samples, the uniaxial compressive strength of the coal increased with the increase in the freezing time, and the uniaxial compressive strength increased 4.02 times compared with that of the original coal samples after freezing for 150 min. The uniaxial compressive strength of TD coal samples continued to increase under different circumferential pressures. After 50 min of LN<sub>2</sub> action, the uniaxial compressive strengths of the 5 MPa and 10 MPa samples were 2.92 and 5.39 times that of the 1 MPa sample. Overall, the uniaxial compressive strength of the coal increased when the coal samples were treated with LN<sub>2</sub> freezing. The uniaxial compressive strength of the coal in the freeze–thaw-state (TR) coal samples tended to increase slowly with the increase in LN<sub>2</sub> treatment time. The uniaxial compressive strength of the TR coal samples increased and then decreased with the increase in the enclosing pressure under different enclosing pressures, and reached its peak value at 5 MPa. With different times of the LN<sub>2</sub> treatment, the uniaxial compressive strengths of the frozen coal samples were always higher than those of the freeze–thawed coal samples due to the increased internal friction between the coal particles caused by the cementing effect of the ice, the water–ice phase transition and the thermal expansion effect caused by the low temperature of LN<sub>2</sub>. The uniaxial compressive strengths of the coal samples in the frozen state were greater than those of the

coal samples in the frozen–thawed state under different circumferential pressures, and the coal samples were damaged to a higher degree after the freeze–thawing treatment, with a higher degree of internal damage and a reduced ability to resist deformation.

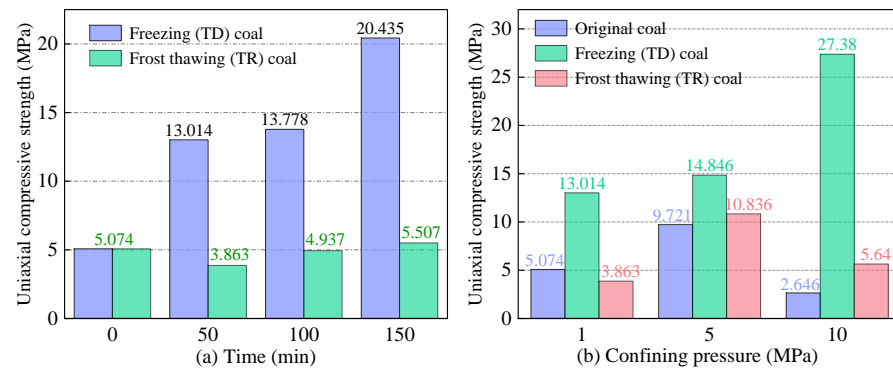


**Figure 4.** Variation in uniaxial compressive strength of coal samples in different states.

#### 4.1.2. Peak Strain Characterization

Peak strain characterizes the maximum amount of axial deformation when the coal sample is ruptured. The larger the peak strain, the larger the amount of axial deformation when the coal sample is ruptured. The peak strains of the frozen and freeze–thawed coal samples after different treatments are shown in Figure 5.

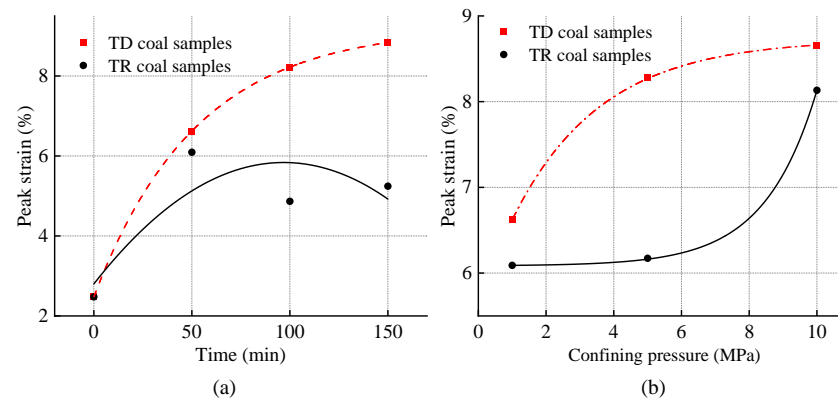


**Figure 5.** Peak strain of coal samples after treatment in different states: (a) same enclosure pressure different time; (b) same time different enclosure pressure.

As shown in Figure 5, uniaxial compression experiments were carried out after the  $\text{LN}_2$  freezing and freezing and thawing of coal samples for different times under 1 MPa circumferential pressure, and from the beginning to the end of the process, the peak strains of TD coal samples and TR coal samples increased by 6.36% and 2.77%, respectively. The loading experiments of the frozen and freeze–thawed coal samples under different enclosure pressures were started after 50 min of  $\text{LN}_2$  freezing, and from the beginning to the end, the peak strains of TD and TR coal samples increased by 2.04% and 2.043%, respectively. During the freezing of the coal with  $\text{LN}_2$ , the coal shrank in the cold and decreased in volume. After the water–ice phase transition, the coal body pores expanded, solid ice completely filled in the pore space, the cementing effect of the ice improved the internal friction between the coal matrix particles, the thermal expansion effect caused by the water–ice phase transition and  $\text{LN}_2$  low-temperature vaporization occurred, and the resistance to deformation was increased. After a longer time of  $\text{LN}_2$  action, the water-saturated coal pore water was all converted into pore ice, the coal pore expansion reached the maximum, the degree of deterioration reached the highest at the time of melting, and the peak strain began to decrease. By fitting the peak strains of the coal samples after different treatments, the following relation was obtained:

$$\varepsilon_1 = 9.22 - 6.74 \times 0.98^t (R^2 = 1) \quad (1)$$

where  $\varepsilon_1$  is the peak strain of TD coal samples with different LN<sub>2</sub> freezing times at 1 MPa surrounding pressure.

$$\varepsilon_2 = 2.80 + 0.06t - 0.0003t^2 (R^2 = 0.71) \quad (2)$$

where  $\varepsilon_2$  is the peak strain of TR coal samples with different LN<sub>2</sub> freezing times at 1 MPa surrounding pressure.

$$\varepsilon_3 = 8.73 - 3.08 \times 0.68^m (R^2 = 0.99) \quad (3)$$

where  $\varepsilon_3$  is the peak strain under different circumferential pressures after 50 min of LN<sub>2</sub> freezing of TD coal samples.

$$\varepsilon_4 = 0.003e^{0.65m} + 6.08 (R^2 = 0.99) \quad (4)$$

where  $\varepsilon_4$  is the peak strain under different circumferential pressures after 50 min of LN<sub>2</sub> freezing of TR coal samples.

#### 4.1.3. Modulus of Elasticity Analysis

The modulus of elasticity is an important physical quantity that measures the ability of an object to resist elastic deformation, and the greater its value, the greater the stress on the material when it undergoes elastic deformation.

Figure 6 shows the change process of the elastic modulus of the coal samples in different states. The modulus of elasticity of the frozen-state (TD) coal samples decreased and then increased after freezing treatment for different times. After 150 min treatment with LN<sub>2</sub>, the growth was 1.13 times of the original. The freeze–thaw state (TR) coal samples, whose modulus of elasticity was consistently lower than that of the original coal samples, first decreased and then increased, and finally showed a decreasing trend. After 150 min of treatment, it was reduced to 46.82% of the original, the elastic modulus of the TD coal samples was always larger than that of TR coal samples under different enclosure pressures, and the trend continued to increase. The elastic modulus of the original coal samples was larger than that of the LN<sub>2</sub>-treated coal samples under 5 MPa enclosure pressure. In the experimental design of the enclosure pressure, 5 MPa enclosure pressure was more suitable for treating the coal samples after 50 min of LN<sub>2</sub> treatment, the frozen and thawed coal samples were more prone to fracture under 1 MPa enclosure pressure, and the frozen coal samples were less prone to deformation under 10 MPa enclosure pressure. With the increase in LN<sub>2</sub> freezing time, the modulus of elasticity of the frozen-state coal samples increased, and the modulus of elasticity of the freeze–thawed-state coal samples decreased, and with the increase in the enclosing pressure, the resistance to deformation of the frozen-state coal samples was enhanced in the TD coal samples and weakened in the TR coal samples after the treatment of the frozen-state coal samples with LN<sub>2</sub>.

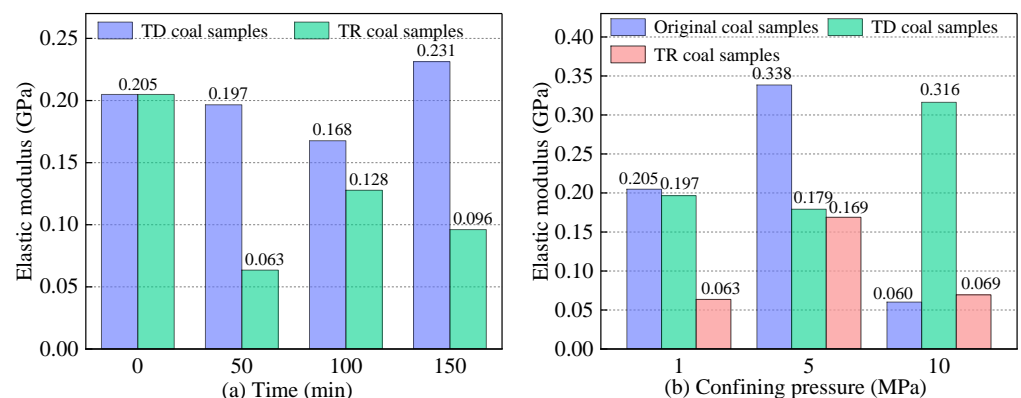


**Figure 6.** Changes in modulus of elasticity of coal samples in different states.

#### 4.1.4. Analysis of Damage Variables and Freezing (Freeze–Thaw) Coefficients

After LN<sub>2</sub> treatment, coal samples undergo subtle changes at the macroscopic and microscopic levels, causing damage to internal mechanics and force properties, and in the experiments, the coal samples produced different damage states at different periods of LN<sub>2</sub> treatment. Taking the state of the original coal samples as a benchmark, the damage characteristics of the coal samples were analyzed in combination with the macroscopic damage theory [32], and the damage variable  $D$  of the coal samples was defined as

$$D = 1 - E/E_0 \quad (5)$$

where  $D$  is the damage variable;  $E$  is the elastic modulus of the coal sample after damage; and  $E_0$  is the elastic modulus of the original coal sample.

Figure 7 shows the changes in the freezing (thawing) damage variables of the coal samples in different states after LN<sub>2</sub> treatment. As can be seen from the figure, after different times of LN<sub>2</sub> treatment, the damage variable of coal samples in the freezing state was negative, and the damage variable of the coal samples in the freezing and thawing state was positive. The main reason for this is the violent conflict between the frozen and shrunken coal after the freezing of LN<sub>2</sub> and the water–ice mixture with an increased volume of the water–ice phase change, and the great localized compressive and tensile stresses between the expanding ice and the coal matrix. The pores of the frozen-state coal samples were filled and the pores of the freeze–thawed-state coal samples dilated, resulting in the production of differences in the freeze–thaw damage variables. The results show that the higher the circumferential pressure is for the coal samples, the smaller the elastic stage of the damage is, and the longer the time of damage.

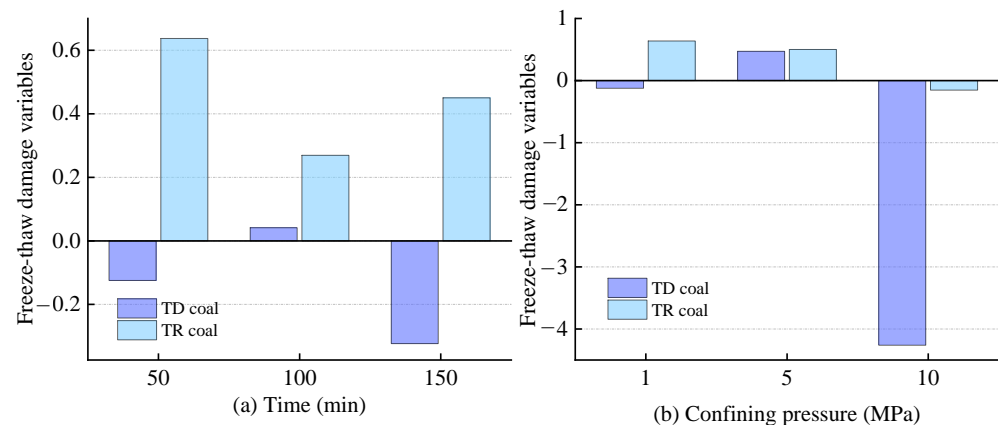


**Figure 7.** Variation in freezing (thawing) damage variables in different states of coal samples.

Rocks themselves have the ability to resist freezing and thawing damage, and coal belongs to a special type of rock. With reference to the Rock Experimentation Procedure for Hydraulic and Water Conservancy and Hydroelectric Engineering (SL264-2001), the freezing (freezing and thawing coefficient) of the coal, which expresses the ability of the coal to resist freezing (freeze–thaw) damage, was defined as follows:

$$K_f = R_f/R_s \quad (6)$$

where  $K_f$  is the coefficient of freezing and thawing,  $R_f$  is the uniaxial compressive strength (MPa) after the freezing (thawing) test, and  $R_s$  is the uniaxial compressive strength (MPa) before the freezing (thawing) test.

From Figure 8, we can obtain the change rule of the freezing and thawing coefficient of coal samples in different states. The freeze–thaw coefficients of the TD and TR coal samples after different times of LN<sub>2</sub> treatment, the freeze–thaw coefficients grew with the increase in the LN<sub>2</sub> action time, but the growth of TR coal samples gradually decreased and the growth of TD coal samples was larger. In the axial pressure application process, the presence of

1 MPa circumferential pressure made the coal circumferential force state change, and the uniaxial compressive strength of the coal increased. The longer the freezing time, the more liquid water was completely converted to solid ice, and the degree of pore filling increased. The freeze–thaw coefficients of both the TD and TR coal samples showed an increase after treatment with different circumferential pressures for the same freezing time. With the increase in circumferential pressure, the coal circumferential force increased, the frozen coal samples needed more axial pressure to destroy the coal samples, and the frozen–thawed coal samples needed more axial pressure to be compacted, so the coefficients of freezing and thawing both increased.

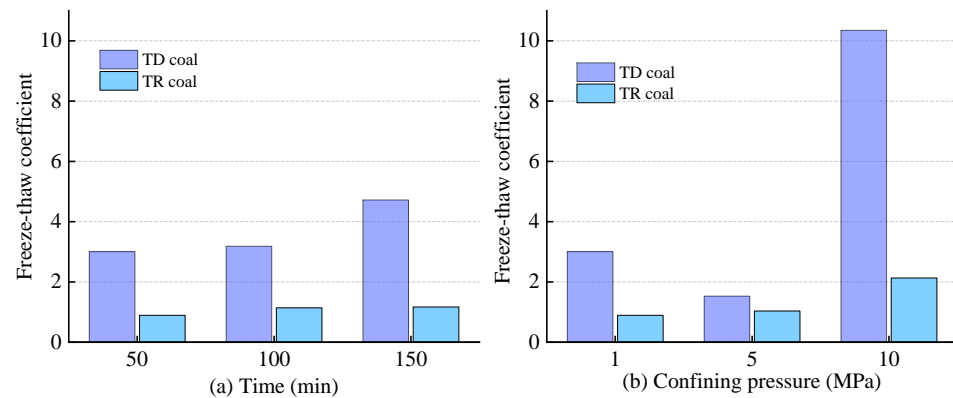


**Figure 8.** Variation in freezing (thawing) coefficient of coal samples in different states.

#### 4.2. Analysis of Deformation Amplitudes during Freeze–Thaw Processes

According to the first law of thermodynamics, the energy received by the coal sample during loading is converted into elastic strain energy as well as damage dissipation energy within the coal sample. The total energy received by the system can be obtained by integrating the stress–strain curve. This is shown in Figure 9.

$$F = D + E \quad (7)$$

where  $F$  is the total energy received by the system,  $D$  is the damage dissipation energy, and  $E$  is the elastic strain energy. In the figure,  $a$  is the compressive limit,  $b$  is the closed strain, and  $c$  is the peak strain.

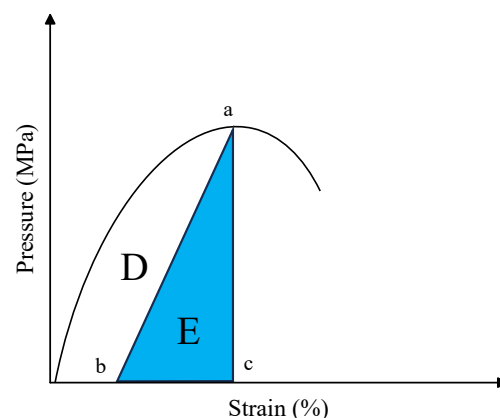


**Figure 9.** Energy profile of coal samples during loading.

After the coal sample reaches the elastic limit, the total energy input to the system reaches the maximum, producing plastic deformation to start rupture, and the coal enters the damage destruction stage. Coal sample rupture is mainly caused by the accumulation of elastic strain energy; the coal sample loses its load-bearing capacity, the accumulated

energy starts to be released, and the input energy of the system is converted into elastic strain energy and dissipated energy in different strain responses.

As can be seen from Figure 10, the elastic strain energy and dissipation energy of the coal samples were changed after different LN<sub>2</sub> treatments. From Figure 10a, it can be seen that the elastic strain energy of TD coal samples was positively correlated with the freezing time before 80 min and negatively correlated after 80 min, and the dissipation energy was the opposite. From the beginning to the end, the elastic strain energy increased by 10.02%. The elastic strain energy of the TR coal samples was positively correlated with the freezing time and negatively correlated with the dissipation energy. From the beginning to the end, the elastic strain energy increased by 31.36%. The longer the LN<sub>2</sub> froze the coal, the higher the degree of coal pore phase change, the increase in coal damage, the increase in dissipation energy, and the decrease in the proportion of elastic strain energy. When damage occurred within a coal sample, the ability to store elastic energy within the sample decreased and the proportion of the total energy input to the sample that was released as dissipated energy increased. From Figure 10b, it can be seen that the elastic strain energy is positively correlated with the freezing time before 6 MPa and negatively correlated after 6 MPa for the TD and TR coal samples, and the dissipation energy is the opposite. From the beginning to the end, the elastic strain energy of the two coal samples decreased by 2% and 4.27%, respectively. With the increase in the circumferential pressure, the coal stress increased. Under the double action of axial and circumferential stress, the coal damage was intensified, the dissipation energy increased, and the percentage of elastic strain energy decreased. By fitting the elastic strain energy and dissipation energy of the coal samples after different treatments, the following relationship was obtained:

$$E_1 = 95.09 - 30.49 \times 0.95^t (R^2 = 0.99) \quad (8)$$

$$E_2 = 65.78 + 0.75t - 0.0047t^2 (R^2 = 0.86) \quad (9)$$

$$D_1 = 4.91 + 30.49 \times 0.95^t (R^2 = 0.99) \quad (10)$$

$$D_2 = 34.22 - 0.76t + 0.0047t^2 (R^2 = 0.86) \quad (11)$$

where  $E_1$ ,  $E_2$  are the elastic strain energies of the TD and TR coal samples, respectively;  $D_1$ ,  $D_2$  are the dissipation energies of the TD and TR coal samples, respectively; and  $t$  is the time of LN<sub>2</sub> action.

$$E_3 = 102.54 - 7.76m + 0.86m^2 (R^2 = 1) \quad (12)$$

$$E_4 = 94.98 - 3.05m + 0.24m^2 (R^2 = 1) \quad (13)$$

$$D_3 = -2.54 + 7.75m - 0.68m^2 (R^2 = 1) \quad (14)$$

$$D_4 = 5.01 + 3.05m - 0.24m^2 (R^2 = 1) \quad (15)$$

where  $E_3$  and  $E_4$  are the elastic strain energies of the TD and TR coal samples,  $D_3$  and  $D_4$  the dissipation energies of the TD and TR coal samples, respectively, and  $m$  is the different enclosure pressures.

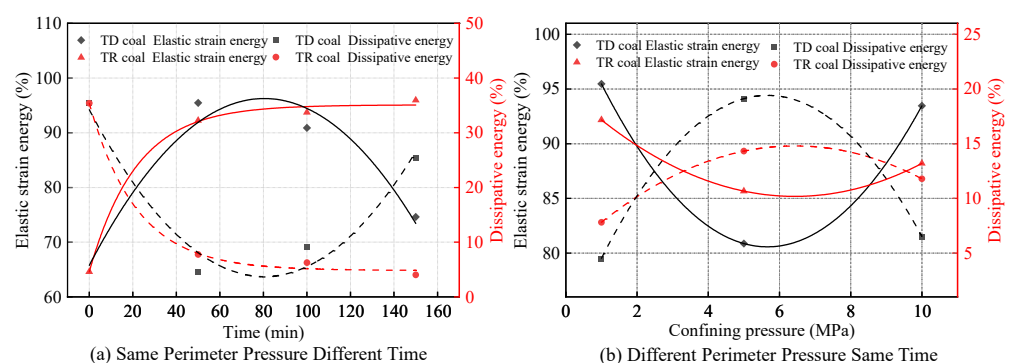


**Figure 10.** Energy evolution of differently treated coal samples during the loading process.

#### 4.3. Mechanism Analysis of LN<sub>2</sub> Action on Coal

In the process of coal formation, many initial pores and fractures are formed at the macro and micro levels of the coal by the interference of many factors. When subjected to force, stress concentration is formed around the micropores and the tip part. When this stress is greater than the limit that the coal can withstand, new fissures will develop along the initial fissures, further new fissures will be formed, the initial pores will be developed and expanded, and the number of pores will grow. In the process of the LN<sub>2</sub> treatment of water-saturated coal samples, first, the pore water in the initial pore fissures of the coal samples undergoes a phase change into solid ice. Due to the different density of water ice, it theoretically produces 0.09-times volume expansion in the process of phase change, which changes the stress in the pore fractures of the coal and produces stress concentration at the tip and the wall of the pore fractures. Secondly, after making contact with LN<sub>2</sub>, the room-temperature coal instantly generates a temperature-gradient difference of 200 °C due to the ultra-low temperature of LN<sub>2</sub> (−196 °C). The coal matrix is subjected to cold volume contraction, and different sizes of pores inside the coal produce different degrees of volume changes. The internal tensile stress inside the coal changes, resulting in the emergence of new fractures inside the coal; the number of pores grows; and the mechanical properties of the coal are reduced. Finally, after the LN<sub>2</sub> enter the pores of the coal body, it undergoes a phase change from liquid to gas, the volume of the coal expands, and pores and cracks of the coal body are developed and expand to the outside of the pore wall under the effect of thermal expansion.

After the LN<sub>2</sub> freezing treatment of water-saturated coal samples, the internal pore water is transformed into pore ice, the initial fractures are expanded under the action of LN<sub>2</sub>, and some of the expanded channels are also filled under the influence of pore ice. Additionally, due to the transformation of the water from liquid to solid, the cementing action of the ice makes the coal brittle, but it also increases the ability of the coal samples to resist deformation when there is a peripheral pressure. During loading, first, the initial pores are compressed and do not deform slowly within the elastic limits. The coal, which becomes hard due to the presence of ice caused by the freezing of LN<sub>2</sub>, requires more stress before it enters into plastic deformation, and destruction occurs after reaching the elastic limit. The total energy of the system does not increase. The coal is subjected to the surrounding pressure during the loading process, which is more in line with the force state of the coal in the coal seam. In our experiment, during loading, the applied circumferential pressure was increased from 1 MPa to 10 MPa, and the stress required for the coal samples to reach the elastic limit was further increased by about 2.1 times. The frozen-state coal samples were converted into frozen–thawed-state coal samples after the internal pore ice was completely thawed, and when the experiment was carried out, there was no longer solid ice in the coal samples and the initial pores inside the coal samples were fully developed and expanded in the initial pressure-dense stage, and the time needed to enter the elastic stage was increased. Applying circumferential pressure, the stress state of the coal changed, the required stress increased, and the uniaxial compressive strength increased correspondingly. At present, the research of LN<sub>2</sub> fracturing technology on coal body fracturing under laboratory conditions is more mature. In future projects, we should also consider the discontinuous deformation of different coal bodies in the coal seam, and carry out laboratory experiments with more simulation of the engineering site (see Figure 11).

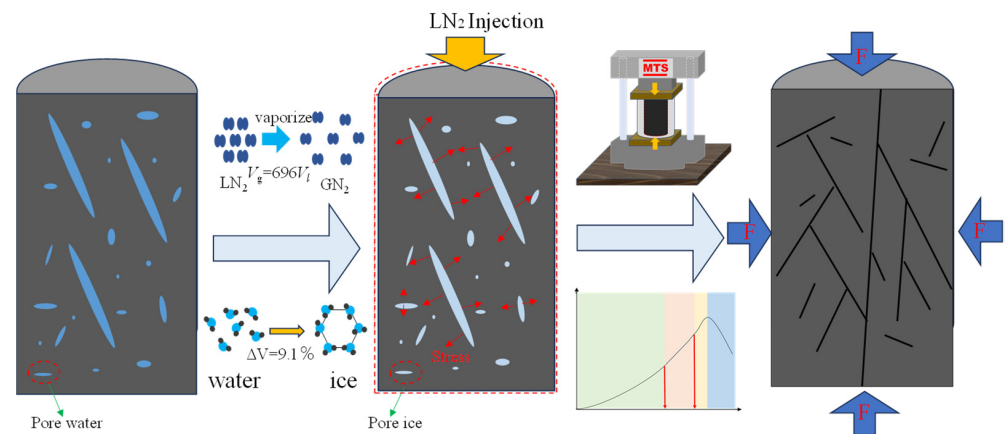


**Figure 11.** Coal fissure evolution process.

## 5. Conclusions

- (1) The uniaxial compressive strength of the frozen coal samples increased and the uniaxial compressive strength of the freeze–thawed coal samples decreased after LN<sub>2</sub> treatment at the same circumferential pressure for different times in the saturated coal. At 150 min, the uniaxial compressive strength of the coal samples was 20.435 MPa in the frozen state and 5.507 MPa in the freeze–thawed state. An increase in uniaxial compressive strength was observed in both the frozen and freeze–thawed coal samples for the same freezing time and different enclosure pressures. The maximum value of 10 MPa for the frozen coal samples was 27.380 MPa, and the maximum of 5 MPa for freeze–thawed coal samples was 10.836 MPa. The increase in the uniaxial compressive strength of the frozen-state coal samples resulted from the increased internal friction between the coal particles due to the cementation of ice.
- (2) The peak strains of the TD and TR coal samples increased by 6.36% and 2.77%, respectively, for the same enclosure pressure with different freezing times. The modulus of elasticity increased to 1.13 times the original and decreased to 46.82% of the original, respectively. The peak strains of TD and TR coal samples increased by 2.04% and 2.043%, respectively, for the same freezing time with different enclosure pressures. The modulus of elasticity of the frozen-state coal samples increased and the modulus of elasticity of the freeze–thaw-state coal samples decreased. Due to the presence of circumferential pressure, the cyclic force of the coal changed during loading and the peak strain increased.
- (3) After the coal reaches its elastic limit, the total energy input to the system is maximized, and the accumulation of elastic strain energy causes rupture damage to the coal. The longer LN<sub>2</sub> freezes the coal, the higher the degree of coal pore phase change, and the more the coal damage increases, the dissipation energy increases, and the proportion of elastic strain energy decreases. The cyclic stress increases, the damage of coal increases, the dissipation energy increases, and the proportion of elastic strain energy decreases.
- (4) In the future application of LN<sub>2</sub> fracturing technology in the field of coal bed methane extraction, the main mechanical principle will be to inject LN<sub>2</sub> through the borehole. After LN<sub>2</sub> enters the pores of the coal, the water in the pores is affected by the temperature and produces a water–ice phase transition, which increases the volume by 0.09 times. Due to the low-temperature damage effect of LN<sub>2</sub>, the temperature difference between the inside and outside of the coal is large, and under the action of the temperature gradient, tensile stress is generated, which makes the stress concentrated in the tip of the pore and the wall of the pore, and produces damage to the coal. LN<sub>2</sub> undergoes liquid–gas phase transition in the pores of the coal, the volume expands in the pores, the pore force state changes, and the strength of the coal is affected. The effect of increasing the permeability of the coal seam around the borehole is achieved

by the above means. The laboratory results we obtained will be used as a reference basis for LN<sub>2</sub> injection parameters.

**Author Contributions:** Methodology, formal analysis, L.Q.; resources, data curation, H.W. and B.L.; visualization, investigation, R.W. and J.L.; validation, R.L. and S.L.; writing—original draft preparation, P.L. All authors have read and agreed to the published version of the manuscript.

**Funding:** This research was funded by the Young Elite Scientist Sponsorship Program by CAST (2022QNRC001), National Natural Science Foundation of China (51904237), International Postdoctoral Exchange Fellowship Program (PC2021064), Innovation Capability Support Program of Shaanxi (2022KJXX-59), Young Talent Fund of Association for Science and Technology in Shaanxi, China (20220437), and China Postdoctoral Science Foundation-funded project (2019M653875XB, 2020T130522).

**Data Availability Statement:** Data are contained within the article.

**Conflicts of Interest:** The authors declare no conflict of interest.

## References

- Zhang, L.; Ponomarenko, T. Directions for Sustainable Development of China's Coal Industry in the Post-Epidemic Era. *Sustainability* **2023**, *15*, 6518. [[CrossRef](#)]
- Teng, J.; Qiao, Y.; Song, P. Analysis of exploration, potential reserves and high efficient utilization of coal in China. *Chin. J. Geophys. Chin. Ed.* **2016**, *59*, 4633–4653. [[CrossRef](#)]
- Wang, A.; Shao, P.; Lan, F.; Jin, H. Organic chemicals in coal available to microbes to produce biogenic coalbed methane: A review of current knowledge. *J. Nat. Gas Sci. Eng.* **2018**, *60*, 40–48. [[CrossRef](#)]
- Li, D.; Luo, P.; Peng, X.; Zhang, B.; Fu, W.; Zou, T.; Fu, L.; Xie, G. Investigation on Pulverized Coal Control Using Calcium Sulfoaluminate Cementitious Proppants in Coalbed Methane Fracturing. *ACS Omega* **2022**, *7*, 8036–8045. [[CrossRef](#)]
- Akhondzadeh, H.; Keshavarz, A.; Awan, F.; Zamani, A.; Iglauer, S.; Lebedev, M. Coal cleat network evolution through liquid nitrogen freeze-thaw cycling. *Fuel* **2022**, *314*, 345–356. [[CrossRef](#)]
- Liu, J.; Yang, T.; Wang, L.; Chen, X. Research progress in coal and gas co-mining modes in China. *Energy Sci. Eng.* **2020**, *8*, 3365–3376. [[CrossRef](#)]
- Ma, H.; Wang, L.; Jia, H.; Chang, J.; Li, Y.; Zhang, X.; Hu, Z.; Yin, Z. Experimental Study on Desorption Characteristics of Coalbed Methane under Variable Loading and Temperature in Deep and High Geothermal Mine. *Adv. Civ. Eng.* **2020**, *2020*, 45–67. [[CrossRef](#)]
- Kang, G.; Kang, T.; Guo, J.; Zhang, R.; Zhang, X.; Zhao, G.; Zhang, B.; Li, L.; Zhang, L. Effect of Electric Potential Gradient on Methane Adsorption and Desorption Behaviors in Lean Coal by Electrochemical Modification Implications for Coalbed Methane Development of Dongqu Mining, China. *ACS Omega* **2020**, *5*, 24073–24080. [[CrossRef](#)]
- Wang, Y.; Feng, W.K.; Hu, R.L.; Li, C. Fracture Evolution and Energy Characteristics During Marble Failure Under Triaxial Fatigue Cyclic and Confining Pressure Unloading (FC-CPU) Conditions. *Rock Mech. Rock Eng.* **2021**, *54*, 799–818. [[CrossRef](#)]
- Liu, S.; Li, X.; Wang, D.; Wu, M.; Yin, G.; Li, M. Mechanical and Acoustic Emission Characteristics of Coal at Temperature Impact. *Nat. Resour. Res.* **2020**, *29*, 1755–1772. [[CrossRef](#)]
- Sass, O. Rock Moisture Fluctuations During Freeze-thaw Cycles: Preliminary Results from Electrical Resistivity Measurements. *Polar Geogr.* **2004**, *28*, 13–31. [[CrossRef](#)]
- Li, Z.; Xu, H.; Zhang, C. Liquid nitrogen gasification fracturing technology for shale gas development. *J. Pet. Sci. Eng.* **2016**, *138*, 253–256. [[CrossRef](#)]
- Mojid, M.; Negash, B.; Abdulelah, H.; Adewumi, K. A state-of-Art review on waterless gas shale fracturing technologies. *J. Pet. Sci. Eng.* **2021**, *196*, 235–246. [[CrossRef](#)]
- Han, S.; Gao, Q.; Cheng, Y.; Han, C.; Xian, Z. Experimental study on brittle response of shale to cryogenic fluid nitrogen treatment. *J. Pet. Sci. Eng.* **2020**, *194*, 56–73. [[CrossRef](#)]
- Chu, Y.; Sun, H.; Zhang, D.; Yu, G. Nuclear magnetic resonance study of the influence of the liquid nitrogen freeze-thaw process on the pore structure of anthracite coal. *Energy Sci. Eng.* **2020**, *8*, 1681–1692. [[CrossRef](#)]
- Lin, H.; Li, J.; Yan, M.; Li, S.; Qin, L.; Zhang, Y. Damage caused by freeze-thaw treatment with liquid nitrogen on pore and fracture structures in a water-bearing coal mass. *Energy Sci. Eng.* **2020**, *8*, 1667–1680. [[CrossRef](#)]
- Memon, K.; Ali, M.; Awan, F.U.R.; Mahesar, A.A.; Abbasi, G.R.; Mohanty, U.R.; Akhondzadeh, H.; Tunio, A.H.; Iglauer, S.; Keshavarz, A. Influence of cryogenic liquid nitrogen cooling and thermal shocks on petro-physical and morphological characteristics of Eagle Ford shale. *J. Nat. Gas Sci. Eng.* **2021**, *96*, 245–265. [[CrossRef](#)]
- Hou, P.; Su, S.; Gao, F.; Liang, X.; Wang, S.; Gao, Y.; Cai, C. Influence of Liquid Nitrogen Cooling State on Mechanical Properties and Fracture Characteristics of Coal. *Rock Mech. Rock Eng.* **2022**, *55*, 3817–3836. [[CrossRef](#)]
- Du, M.; Gao, F.; Cai, C.; Su, S.; Wang, Z. Study on the surface crack propagation mechanism of coal and sandstone subjected to cryogenic cooling with liquid nitrogen. *J. Nat. Gas Sci. Eng.* **2020**, *81*, 456–478. [[CrossRef](#)]

20. Cai, C.; Gao, F.; Yang, Y. The effect of liquid nitrogen cooling on coal cracking and mechanical properties. *Energy Explor. Exploit.* **2018**, *36*, 1609–1628. [[CrossRef](#)]
21. Wang, X.; Qi, X.; Ma, H.; Gao, K.; Li, S. Experimental study on freeze–thaw damage characteristics of coal samples of different moisture contents in liquid nitrogen. *Sci. Rep.* **2022**, *12*, 18543. [[CrossRef](#)] [[PubMed](#)]
22. Su, S.; Hou, P.; Gao, F.; Gao, Y.; Cai, C.; Zhang, Z.; Liang, X. A fractal perspective on structural damage and feature characteristics of coal subjected to liquid nitrogen at laboratory-scale. *Fractals* **2022**, *30*, 134–145. [[CrossRef](#)]
23. Zhao, Y.; Song, H.; Liu, S.; Zhang, C.; Gao, F. Mechanical anisotropy of coal with considerations of realistic microstructures and external loading directions. *Int. J. Rock Mech. Min. Sci.* **2019**, *116*, 111–121. [[CrossRef](#)]
24. Li, Z.; Zhang, G. Fracture Segmentation Method Based on Contour Evolution and Gradient Direction Consistency in Sequence of Coal Rock CT Images. *Math. Probl. Eng.* **2019**, *2019*, 123–141. [[CrossRef](#)]
25. Qin, L.; Zhai, C.; Liu, S.; Xu, J.; Tang, Z.; Yu, G. Failure Mechanism of Coal after Cryogenic Freezing with Cyclic Liquid Nitrogen and Its Influences on Coalbed Methane Exploitation. *Energy Fuels* **2016**, *30*, 8567–8578. [[CrossRef](#)]
26. Zhou, C.; Gao, F.; Cai, C.; Zheng, W.; Huo, L. Mechanical Properties and Damage Evolution of Heated Granite Subjected to Liquid Nitrogen Cooling. *Appl. Sci.* **2022**, *12*, 10615. [[CrossRef](#)]
27. Du, M.; Gao, F.; Cai, C.; Su, S.; Wang, Z. Experimental Study on the Damage and Cracking Characteristics of Bedded Coal Subjected to Liquid Nitrogen Cooling. *Rock Mech. Rock Eng.* **2021**, *54*, 5731–5744. [[CrossRef](#)]
28. Akhondzadeh, H.; Keshavarz, A.; Awan, F.U.R.; Ali, M.; Al-Yaseri, A.; Liu, C.; Yang, Y.; Iglauer, S.; Gurevich, B.; Lebedev, M. Liquid nitrogen fracturing efficiency as a function of coal rank: A multi-scale tomographic study. *J. Nat. Gas Sci. Eng.* **2021**, *95*, 345–367. [[CrossRef](#)]
29. Tatone, B.; Abdelaziz, A.; Grasselli, G. Novel Mechanical Classification Method of Rock Based on the Uniaxial Compressive Strength and Brazilian Disc Strength. *Rock Mech. Rock Eng.* **2022**, *55*, 2503–2507. [[CrossRef](#)]
30. Chu, Y.; Zhang, D.; Liu, H.; Wu, X.; Zhai, P.; Sheng, T. Experimental study on mechanical properties, acoustic emission characteristics and energy evolution of coal samples after freezing with liquid nitrogen. *Fuel* **2022**, *5*, 321–333. [[CrossRef](#)]
31. Qin, L.; Ma, C.; Li, S.; Lin, H.; Ding, Y.; Liu, P.; Wang, P.; Gao, Z. Liquid Nitrogen’s Effect on the Mechanical Properties of Dried and Water-Saturated Frozen Coal. *Energy Fuels* **2022**, *36*, 1894–1903. [[CrossRef](#)]
32. Bonetti, E.; Fremond, M. Damage theory: Microscopic effects of vanishing macroscopic motions. *Comput. Appl. Math.* **2003**, *22*, 134–143. [[CrossRef](#)]

**Disclaimer/Publisher’s Note:** The statements, opinions and data contained in all publications are solely those of the individual author(s) and contributor(s) and not of MDPI and/or the editor(s). MDPI and/or the editor(s) disclaim responsibility for any injury to people or property resulting from any ideas, methods, instructions or products referred to in the content.